Report

Current Biology

Binocular Visual Responses in the Primate Lateral Geniculate Nucleus

Graphical Abstract

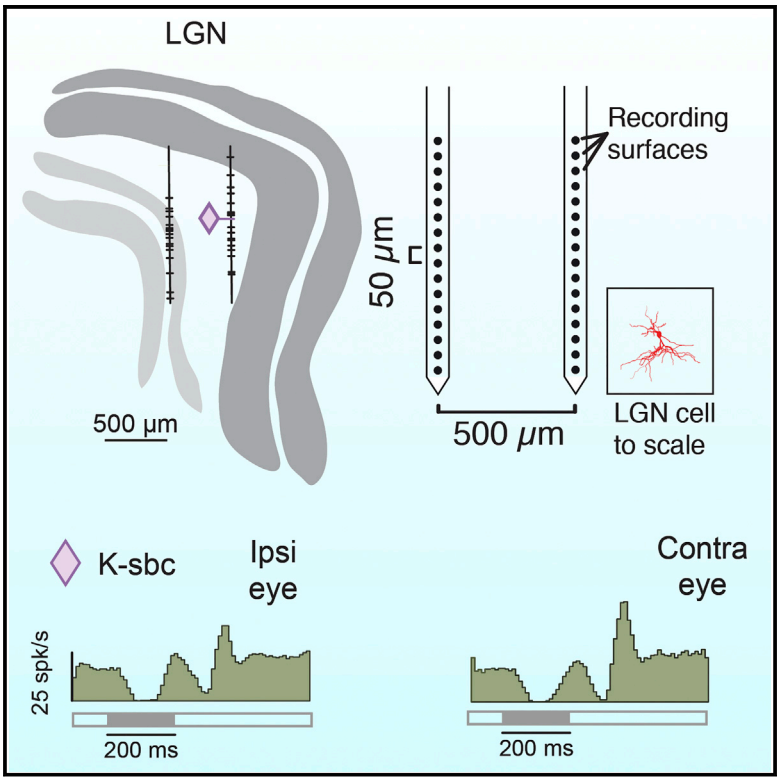

Authors

Natalie Zeater, Soon K. Cheong, Samuel G. Solomon, Bogdan Dreher, Paul R. Martin

Correspondence

prmartin@sydney.edu.au

In Brief

In primates, the dorsal lateral geniculate nucleus (LGN) is a laminated structure, where each layer gets visual input from one eye. Zeater et al. show that many neurons located between the main LGN layers get binocular visual inputs, giving primate LGN a feature in common with simpler visual systems of non-primate mammals such as rodents.

Highlights

- Some neurones in marmoset lateral geniculate nucleus (LGN) show binocular responses
- Binocular responses are found in the evolutionary ancient koniocellular layers of LGN

Zeater et al., 2015, Current Biology *25*, 1–6
December 21, 2015
http://dx.doi.org/10.1016/j.cub.2015.10.033

CellPress

Please cite this article in press as: Zeater et al., Binocular Visual Responses in the Primate Lateral Geniculate Nucleus, Current Biology (2015), http://dx.doi.org/10.1016/j.cub.2015.10.033

Current Biology
Report

Binocular Visual Responses in the Primate Lateral Geniculate Nucleus

Natalie Zeater,[1,2,3] Soon K. Cheong,[1,2,5] Samuel G. Solomon,[2,4] Bogdan Dreher,[2] and Paul R. Martin[1,2,3,*]
[1]Save Sight Institute, The University of Sydney, Sydney, NSW 2000, Australia
[2]School of Medical Sciences, The University of Sydney, Sydney, NSW 2000, Australia
[3]ARC Centre of Excellence for Integrative Brain Function, University of Sydney, Sydney, NSW 2000, Australia
[4]Department of Experimental Psychology, University College London, London WC1P 0AH, UK
[5]Present address: Flaum Eye Institute, University of Rochester, Rochester, NY 14627, USA
*Correspondence: prmartin@sydney.edu.au
http://dx.doi.org/10.1016/j.cub.2015.10.033

SUMMARY

The dorsal lateral geniculate nucleus (dLGN) in carnivores and primates is a laminated structure, where each layer gets visual input from only one eye [1, 2]. By contrast, in rodents such as mice and rats, the dLGN is not overtly laminated, the retinal terminals from the two eyes are only partially segregated [3, 4], and many cells in the binocular segment of dLGN get excitatory inputs from both eyes [5, 6]. Here, we show that the evolutionary ancient koniocellular (K) division of primate dLGN, like rodent dLGN, forms a subcortical site of binocular integration. We recorded single-cell activity in dLGN of anesthetized marmoset monkeys. As expected, cells in the parvocellular (P) and magnocellular (M) layers received monocular excitatory inputs. By contrast, many cells in the K layers received excitatory inputs from both eyes. The specialized properties of distinct K sub-populations (for example, blue-yellow color selectivity) were preserved across the two eye inputs, and where tested, the contrast sensitivity of each eye input was roughly matched. The results argue that evolutionarily widely separated orders such as rodents and primates have a shared strategy of integrating signals from the two eyes in subcortical circuits.

RESULTS

The K layers of the primate dorsal lateral geniculate nucleus (dLGN) contain multiple neuronal types that transmit diverse visual signals to visual cortices. For example, distinct types of koniocellular (K) cells show color-selective "blue-on" (K-bon), "blue-off" (K-boff), "orientation-selective" (K-o) cells, and "suppressed-by-contrast" (K-sbc) properties [7–10]. We have found that binocular convergence is widespread among K cells, indicating a fundamental difference in functional organization to that of parvocellular (P) cells and magnocellular (M) cells.

Characteristics of Binocular Responses

Figure 1 shows an example multi-electrode array penetration through the dLGN (Figures 1A and 1B) and single-cell action potentials (spikes) recorded during monocular stimulation through each eye, across two 500-s recording epochs separated by ~35 min (Figure 1C). Across these records, spike amplitude shows a small systematic drift, but spike shape remains consistent (Figure 1C, upper panels), and principal-component (PC) analysis (Figure 1C, lower panels) shows invariant cluster position relative to background activity, indicating stable recording from a single isolated neuron. Figure 1D shows an example trajectory from a second animal, and Figures 1E–1I show example peri-stimulus time histograms (PSTHs) from cells recorded in this penetration. Monocular visual responses shown in Figures 1E–1G were typical of most (57/80) cells encountered. A proportion of cells, however (23/80; 29%; e.g., Figures 1H and 1I), respond in the same way to stimuli presented through either eye. These binocular responses are evident for both optimal (left PSTHs) and sub-optimal stimuli (right PSTHs). The presence of simultaneously recorded monocular and binocular cells, at the same recording site (Figures 1, S1, and S2), indicates that eye occlusion was effective, for all cells would respond if light were leaking into the occluded eye.

Functional Weight of Binocular Inputs

We next asked how the functional weight of non-dominant eye responses is distributed across different dLGN populations. As expected [1, 11, 12], P cells and M cells (Figures 2A and 2B; Table S1) are suppressed by, or respond only feebly to, non-dominant eye stimulation. Vigorous (>10 spikes/s) binocular responses are restricted almost exclusively to K cells (Figures 2C and 2D; Table S1). Analysis of spike rates (Figures 2G–2I; see the Experimental Procedures) shows the mean weight of non-dominant input to K cells (0.14; SD 0.20) and M cells (0.05; SD 0.07) is greater than zero ($p < 0.01$; Kolmogorov-Smirnov test), but that of P cells is not (−0.02; SD 0.12).

The broad distribution of eye dominance in K cells reflects presence of K cells with strong excitatory inputs from both eyes; for example, 22/51 (43%) of K cells have non-dominant weight above 0.2, whereas only one P cell does and no M cells do (Figure 2I). Binocular excitatory convergence is apparent in all K cell sub-populations that we recorded (Table S1). Despite the bimodal appearance of the K cell histogram (Figure 2I), the non-dominant weight distribution does not depart from

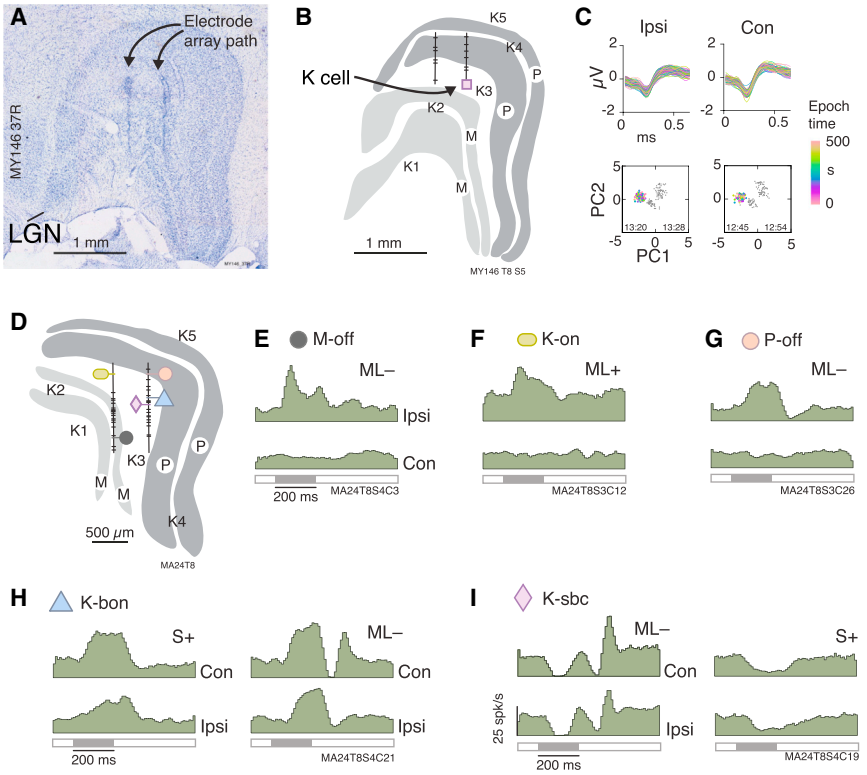

Figure 1. Analysis of Binocular Inputs to K Cells

Electrophysiological recordings from K layers are challenging because the K layers are thin and K cells are small. Therefore, we used multi-electrode arrays to improve the yield of K cells.

(A) Micrograph of a Nissl-stained coronal section through marmoset dorsal lateral geniculate nucleus (dLGN) including the trajectory of an array penetration (case MY146).

(B) Schematic drawing of this section showing the parvocellular (P, dark gray) and magnocellular (M, light gray) layers surrounded by koniocellular (K, white) layers. Black vertical lines and horizontal tick marks show reconstructed positions of cells recorded at a single array location. Square symbol marks a K layer recording position.

(C) Top: spike waveforms recorded at the position marked by the symbol in (B). Spikes were uniformly sampled across a 500-s epoch of monocular stimulus presentation through ipsilateral (Ipsi, left) or contralateral (Con, right) eye. Bottom: principal-component (PC) analysis of thresholded 0.6 ms voltage windows at the recording site show separation of the isolated unit (color-coded points) from other units and background "hash" activity (gray points). Recording start and end times are indicated at the bottom of each panel. A full reconstruction of this recording trajectory is shown in Figure S1.

(D) Reconstructed trajectory though the dLGN of a different animal (case MA24). Colored symbols mark the single units with responses illustrated in (E)–(I).

(E) Peri-stimulus time histograms (PSTHs) of responses of a magnocellular (M) off-center unit to stimuli delivered through the Ipsi or Con eye. Responses to 200-ms contrast pulses are shown. Pulse duration is indicated by the dark bar beneath each PSTH. Cone modulation direction is indicated to right of each PSTH. This cell shows monocular response to decrements in medium/long-wave sensitive cone activity (ML−).

(F) Koniocellular on-center (K-on) cell showing monocular responses to ML cone increments (ML+).

(G) Parvocellular off-center (P-off) cell showing monocular responses to ML−.

(H) Koniocellular blue-on cell (K-bon) showing binocular excitatory responses to short-wave sensitive cone increments (S+, right) and ML− (left).

(I) Koniocellular suppressed-by-contrast (K-sbc) cell showing binocular transient suppression following onset and offset of ML− (left) and sustained suppression for S cone increments (S+, right).

Scale bars in (E) apply to (B)–(F). Full details of response properties and spike sorting for these cells are shown in Figure S2.

unimodality for any cell group (Hartigan unimodality test: P, $p = 0.89$; M, $p = 0.72$; K, $p = 0.76$). We conclude that many K cells receive robust inputs from the non-dominant eye.

Response Latency

If non-dominant eye signals reach K cells through a longer nerve pathway and/or more synaptic relays than dominant eye responses do, then we would expect them to always appear at longer latency. As expected [13], peak response latency of dominant eye responses of K cells (mean 61.5 ms; SD 30.1; $n = 51$) was significantly longer than that of M cells (37.2 ms; SD 16.5; $n = 13$; $p < 0.01$) and marginally longer than that of P cells (52.8 ms; SD 22.1; $n = 16$; $p = 0.24$). We analyzed response latency for K cells showing >5 spikes/s excitatory response to non-dominant eye stimulation (Figures 2E and 2F). Across these cells, the mean latency for non-dominant eye stimulation (80.5 ms; SD 38.3; $p = 0.03$) is ~20 ms longer than latency for dominant eye stimulation (59.0 ms; SD 26.0; $n = 22$; $p = 0.03$). Interocular time lag is not correlated with non-dominant weight ($r^2 = 0.09$; $p = 0.22$). We conclude that non-dominant eye inputs for many (but not all) K cells are delayed relative to dominant eye inputs.

Contrast Sensitivity

Responses described above were to high-contrast stimuli. We asked whether binocular inputs to K cells are also modulated in more-natural environments, where contrast is variable and, on average, low [14]. At two sites, we measured contrast sensitivity for 5 Hz temporal modulation of a spatially uniform achromatic field (Figure 3). The measured K cells show roughly matched contrast-response relation for each eye's input. The first Fourier harmonic of responses was fit to a saturating hyperbolic ("Naka-Rushton") function [15]: $R_c = R_0 + R_{max}c/(c_{50} + c)$, where R is spike rate, c is stimulus contrast, R_0 is maintained spike rate, R_{max} is maximum response, and c_{50} is the contrast at half-maximum response. For K cells ($n = 10$), we found high correlation of the R_{max} parameter for dominant and non-dominant eye stimulation ($r^2 = 0.86$; $p < 0.01$; Figure 3G) and weaker correlation of response gain (R_{max}/c_{50}; $r^2 = 0.44$; $p = 0.04$; data not shown). Thus, for K cells receiving inputs from both eyes, the input is roughly balanced over a range of image contrasts. These data also provide two further clues regarding response timing of binocular inputs. First, mean interocular phase lag at the stimulus frequency (5 Hz) is equivalent to 55.6 ms (SD 9.5; $n = 5$); this value

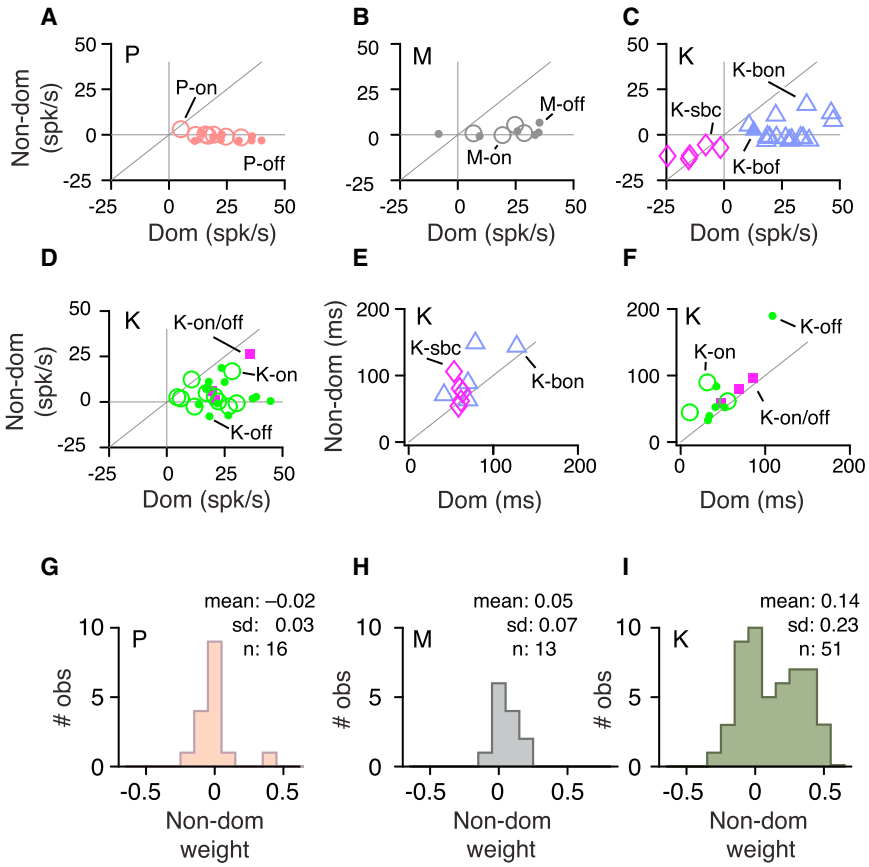

Figure 2. Summary of Binocular Response Properties

(A and B) Scatterplots showing peak firing rates of P cells and M cells for stimuli delivered through dominant (Dom) or non-dominant (Non-dom) eye. Note that on- and off-center P (P-on and P-off) and on- and off-center M (M-on and M-off) cells show only weak influence of the non-dominant eye.

(C and D) Responses of different classes of K cells showing variable excitatory responses to non-dominant stimulation: K blue-on (K-bon); K blue-off (K-bof); K suppressed-by-contrast (K-sbc); K on-center (K-on); K off-center (K-off); and K on/off (K-on/off).

(E and F) Time to peak response following stimulus onset for K cells. Only cells showing >5 spikes/s response to non-dominant stimulation are shown. Response amplitude of K-sbc cells was inverted for this analysis. Note variable delay in response to non-dominant stimulation.

(G–I) Functional weight of non-dominant eye inputs for P, M, and K cells. Note that many K cells get substantial excitatory input from the non-dominant eye.

is broadly consistent with mean lag for pulsed stimuli (~20 ms). Second, response phase is largely independent of response amplitude (Figures 3C, 3D, and 3H); thus, response amplitude cannot explain latency differences between the two eye inputs.

Binocular Integration

At two sites, we held recordings long enough to measure responses to stimuli delivered separately through each eye and also with both eyes open (Figure S3). Binocular interaction was estimated by comparing spike rates in 10-ms bins across 200 ms following preferred stimulus onset for five K cells. Binocular stimulation causes on average mild decreases in spike rate compared to dominant eye stimulation (mean ratio binocular/dominant: 0.86; SD 0.87; n = 5). The binocular spike rate is lower than that predicted by summation of responses to monocular stimulation ([dominant + non-dominant] / dominant: 1.60; SD 0.44; p = 0.18). Three K cells showed strong binocular inputs, evidenced by high correlation between dominant and non-dominant eye responses (r^2 0.70, 0.42, and 0.42; p < 0.01 in each case). Responses of these cells to binocular stimulation (measured ratios 0.80, 0.00, and 0.72) likewise fall below the summed responses to monocular stimulation (predicted ratios 1.91, 1.39, and 2.05). In sum, our data are consistent with sublinear or suppressive binocular integration of K cell responses.

Functional Specificity of Binocular Inputs

The example PSTHs (Figures 1 and S1–S3) suggest that the distinct response signatures of K cells (e.g., K-bon versus K-sbc) are common to both eye inputs. To quantify this observation, we measured spike rate correlations for dominant and non-dominant eye responses (see the Experimental Procedures). For K cells showing non-dominant weight >0.2 (n = 19), we compared the veridical correlation to that obtained by synthetic correlation with responses of other K cells (Figure 4). The measured correlation (main diagonal; Figure 4) was over 8-fold greater than the mean value of synthetic correlation with cells of different functional subtype (mean ratio 8.56; SD 5.81; n = 19; p < 0.01; paired Wilcoxon test) and was also greater than synthetic correlation with members of the same K cell subtype (mean ratio 2.41; SD 0.78; p < 0.01). Both results lead to the conclusion that the specialized properties of K cell subtypes are retained for each eye's inputs.

DISCUSSION

Sources of Binocular Inputs to K Cells

The obvious potential sources of binocular inputs to K cells are (1) convergent direct retinal input, (2) inputs from other subcortical visual centers, and (3) inputs from primary visual cortex. These three main possibilities need to be weighed up in light of our most intriguing finding, that is, the specialized properties of K subtypes are similar in the two eye inputs—a result that implies functional specificity rather than indiscriminate mixing of visual signals.

Anatomically, retinal inputs to K layers do not show the strict eye segregation that defines the P and M layers [16]. Additionally, subcortical inputs to dLGN from the superior colliculus and the parabigeminal nucleus selectively target K layers [17, 18], and many neurons in those areas show binocular excitatory convergence [19–21]. Corticofugal axons likely carry binocular signals, but they make synapses in all layers of the

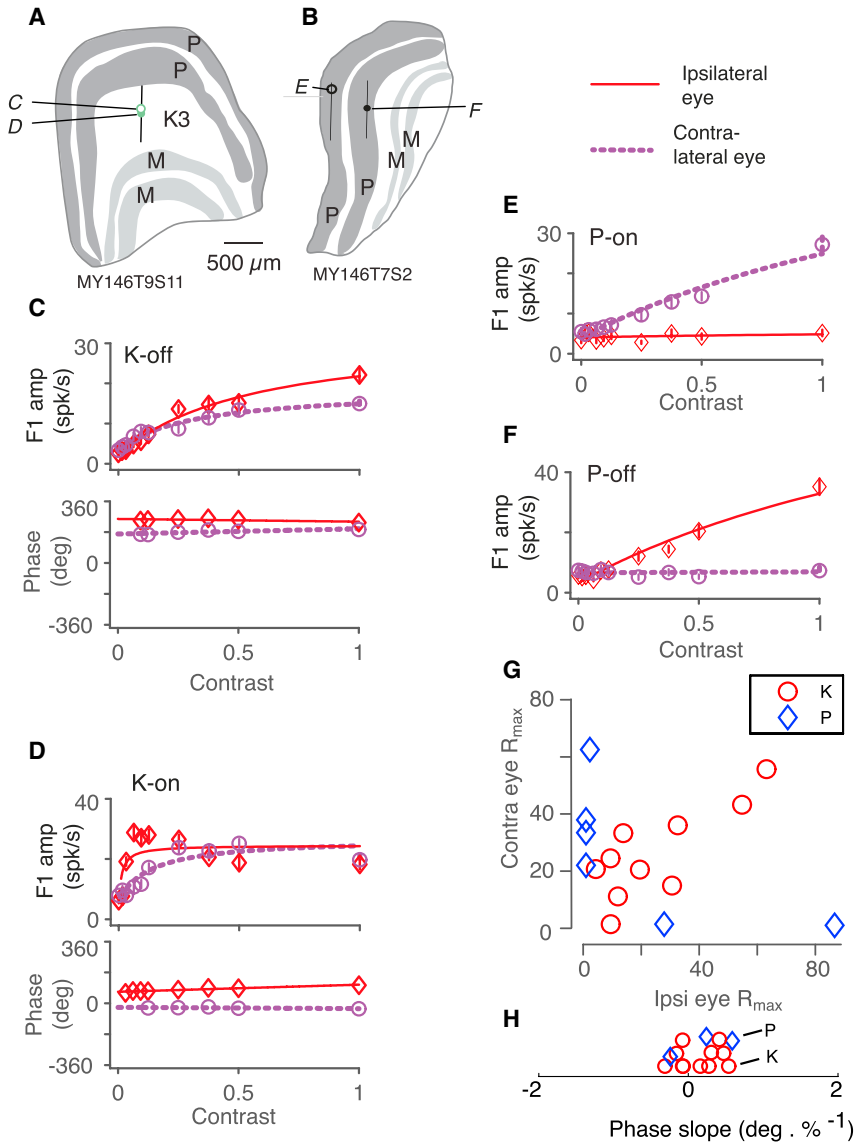

Figure 3. Contrast Sensitivity in Monocular and Binocular dLGN Cells

(A) Reconstructed recording site in layer K3. Recording positions of two K cells are indicated.

(B) Reconstructed recording site in P layers. In this recording, the lateral electrode shank was located in the external (contralateral eye-recipient) P layer and the medial shank was located in the internal (ipsilateral eye-recipient) P layer.

(C and D) Contrast-response functions of K cells for 5 Hz spatial uniform sine intensity modulation. Top: fundamental Fourier component (F1) amplitude. Lines show saturating hyperbolic fits as described in the text. Bottom: F1 phase. Lines show linear regression. These K cells show roughly matched contrast-response functions for stimuli delivered through either eye.

(E and F) Two example P cells showing monocular responses consistent with expected eye input to P layers.

(G) Scatterplot of maximum response amplitude (R_{max}) for contralateral (Contra) and ipsilateral (Ipsi) contrast-varying stimuli.

(H) Slope of linear fits to response phase. Note values are clustered around zero slope, indicating little influence of response amplitude on response timing.

Error bars in (C)–(F) show the SEM.

dLGN and therefore should influence P cells and M cells as well as K cells. These results imply retinal and/or subcortical visual centers as the most likely sources of binocular responses in K cells.

Functional Role of Binocular Integration in K Cells

It seems unlikely that binocular K cells could serve stereoscopic single vision—which relies on orientation-selective inputs from the two eyes [22, 23]—because K cells very rarely show orientation selectivity [24]. Most of our data were collected using a spatially uniform stimulus, in order to rapidly characterize the amplitude and timing of eye inputs, and we have not yet made a parametric study of interocular phase dependence. It is worth noting here that, in cat dLGN, the rarely encountered binocular cells are not sensitive to retinal disparities [25].

But if binocular convergence in K cells does not serve disparity detection, what is its significance? Our hypothesis is that the significance lies in connections of the K layers with midbrain centers regulating spatial attention and orienting [17, 18]. For example, the connections of K layers with parabigeminal nucleus and superior colliculus have homologies to the isthmic nuclei/tectal loops of non-mammalian vertebrates [26, 27]. In birds, this circuit constitutes a subcortical site for binocular integration, allowing response selection among competing visual stimuli [26, 27]. In primates, connections of the parabigemino-tectal circuit to K layers and thence to primary [28–30] and association cortices [31, 32] would give these signals access to brain circuits for higher-level form and motion analysis.

Binocular Processing in Rodents and Primates

Our results add to other points of similarity between the K layers in primate dLGN and the binocular segment of the dLGN of the best-studied rodent species (rats and mice). First, in both systems, many cells respond to complex stimulus features [6, 11, 24, 33–37] (but see also [38]). Second, afferent cortical projections of both systems extend beyond primary visual cortex [4, 31, 32, 39, 40] and target both supra-granular and granular cortical layers [4, 29, 30, 41]. Third, both systems have connections with other subcortical visual centers, including centers regulating attention and vigilance [17, 18, 40, 42, 43]. These homologies suggest that the main P and M layers have been selectively expanded from a primordial subcortical system that serves low-acuity visual functions, including visually guided approach and avoidance behaviors. We conclude that the most obvious

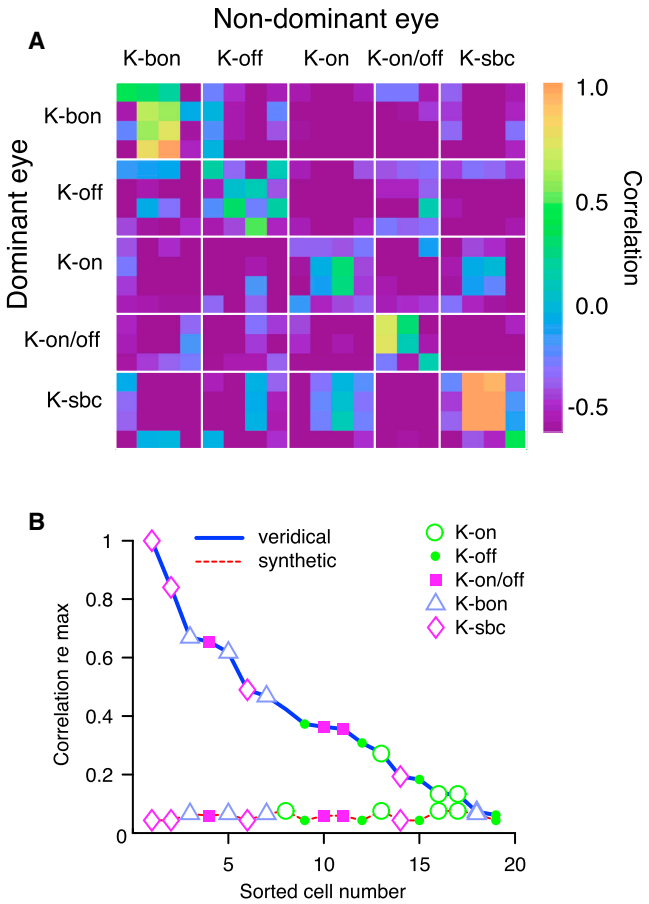

Figure 4. Functional Specificity of Non-dominant Eye Inputs

(A) Correlation matrix. Dominant and non-dominant eye responses were correlated in 10-ms bins during 400 ms following stimulus onset, across four different pulse stimulus conditions (S-cone increment, S-cone decrement, ML-cone increment, and ML-cone decrement). Stimulus duration is 200 ms. Field size is 12°. Elements on the main diagonal show measured (veridical) correlation of dominant eye response amplitude with non-dominant eye response amplitude. Other elements show synthetic correlation between dominant eye responses (taken row-wise) with non-dominant eye responses (taken column-wise) across all other possible combinations of responses in the sample. White lines divide cells of the same functional group: koniocellular blue on/yellow off (K-bon); K-off; K-on; koniocellular on-off field (K-on/off); and K-sbc.

(B) The solid line shows veridical correlation values sorted according to correlation strength. The dashed line shows the mean value for synthetic correlation across all other cells.

purpose of strict eye segregation in the main P and M layers is to deliver monocular signals to the cortex, allowing high-order image properties including retinal disparity to be extracted.

EXPERIMENTAL PROCEDURES

Recordings were made from sufentanil-anesthetized adult marmosets (*Callithrix jacchus*; two male and one female) as described [10, 13]. Experiments conformed to the Australian code for care and use of animals for scientific purposes and were approved by the local institutional committee. Recordings were made with a two-shank silicon array probe (NeuroNexus 16x2); each shank (0.5 mm separation) provided 16 recording surfaces at 50-μm spacing (Figure S2). Each array advance movement was followed by minimum 30 min settle time. Voltage records were sorted (Plexon offline sorter) and analyzed using MATLAB (MathWorks). Spike shape, refractory period criteria (less than two spikes in <2 ms) and cluster quality metrics (multivariate ANOVA; Dunn index) aided single-cell isolation. Cells recorded on more than one channel were reduced to a single data stream (Figures S1 and S2). The P, M, and K layers were identified by combination of anatomical track reconstruction, eye dominance, and responses to cone-isolating stimuli (Figures 1 and S2). On these criteria, recording sites of 71 cells were reconstructed. The location of one site (case MA025, site 1) was not reconstructed; here, five K cells were identified by response signature. Recordings targeted mid-peripheral (5°–15°) binocular visual field representation.

Stimuli comprised temporal square-wave intensity and/or chromaticity modulation of a circular field of diameter 12°–27° ("pulse") delivered by a CRT monitor refreshed at 100 Hz (mean intensity ~50 cd m^{-2}). Short-wave sensitive (S) and medium/long-wave sensitive (ML) cone-isolating pulses (duration 200 ms; 100 repetitions; inter-stimulus interval 600 ms) were constructed by convolving marmoset cone spectral sensitivity with the spectral distribution of monitor phosphors [13]. Spatial uniform 5 Hz sinusoidal modulation of an achromatic field of variable contrast was also presented (stimulus duration 2 s; inter-stimulus interval 2.5 s; 20–60 cycles presented) at two sites. The non-stimulated eye was occluded with a shutter. Responses to pulse stimuli were recorded with two eyes open at two sites (Figure S3).

PSTHs (bin width 10 ms; three-bin moving average) were constructed. Dominant eye and optimal stimulus were assigned as the eye/contrast combination that produced greatest response variance. Maintained firing rate during 100-ms preceding stimulus onset was subtracted from peak (for excitatory responses) or trough (for suppressive responses) of the PSTH. Suppressive responses thus have negative sign. Response latency was calculated as time from stimulus onset to peak or trough of the PSTH. Amplitude of non-dominant response was measured at time of dominant eye response peak. Non-dominant response amplitude was divided by the summed unsigned values of dominant and non-dominant response. This ratio (non-dominant weight) varies between −0.5 and +0.5, where 0 indicates no influence of non-dominant eye stimulation, −0.5 indicates complete response suppression, and the asymptotic value +0.5 indicates equal excitatory response to dominant and non-dominant eye stimulation.

Unless otherwise stated, the Wilcoxon rank-sum test was used for statistical comparisons.

SUPPLEMENTAL INFORMATION

Supplemental Information includes three figures and two tables and can be found with this article online at http://dx.doi.org/10.1016/j.cub.2015.10.033.

AUTHOR CONTRIBUTIONS

N.Z., S.K.C., S.G.S., B.D., and P.R.M. designed the research; N.Z., S.K.C., S.G.S., and P.R.M. collected data; N.Z., S.K.C., S.G.S., B.D., and P.R.M. analyzed data; and N.Z., B.D., S.G.S., and P.R.M. wrote the paper.

ACKNOWLEDGMENTS

We thank A. Pietersen and S.S. Solomon for help with data acquisition; W. Dobbie for programming; and A. Demir, C. Focke, and C. Guy for technical and administrative assistance. We thank U. Grünert, P. Gong, N. Priebe, B. Scholl, and the anonymous reviewers for helpful comments. Support was provided by Australian National Health and Medical Research Council grants 1027913 and 1005427 and Australian Research Council grant CE140100007.

Received: May 19, 2015
Revised: September 30, 2015
Accepted: October 14, 2015
Published: November 19, 2015

REFERENCES

1. Wiesel, T.N., and Hubel, D.H. (1966). Spatial and chromatic interactions in the lateral geniculate body of the rhesus monkey. J. Neurophysiol. *29*, 1115–1156.

2. Casagrande, V.A., and Norton, T.T. (1991). Lateral geniculate nucleus: a review of its physiology and function. In The Neural Basis of Visual Function, A.G. Leventhal, ed. (Macmillan Press), pp. 41–84.
3. Reese, B.E. (1988). 'Hidden lamination' in the dorsal lateral geniculate nucleus: the functional organization of this thalamic region in the rat. Brain Res. Rev. *13*, 119–137.
4. Leamey, C.A., Protti, D., and Dreher, B. (2008). Comparative survey of the mammalian visual system with reference to the mouse. In Eye, Retina, and Visual System of the Mouse, L.M. Chalupa, and R.W. Williams, eds. (MIT Press), pp. 35–60.
5. Grieve, K.L. (2005). Binocular visual responses in cells of the rat dLGN. J. Physiol. *566*, 119–124.
6. Howarth, M., Walmsley, L., and Brown, T.M. (2014). Binocular integration in the mouse lateral geniculate nuclei. Curr. Biol. *24*, 1241–1247.
7. Irvin, G.E., Norton, T.T., Sesma, M.A., and Casagrande, V.A. (1986). W-like response properties of interlaminar zone cells in the lateral geniculate nucleus of a primate (*Galago crassicaudatus*). Brain Res. *362*, 254–270.
8. Szmajda, B.A., Buzás, P., Fitzgibbon, T., and Martin, P.R. (2006). Geniculocortical relay of blue-off signals in the primate visual system. Proc. Natl. Acad. Sci. USA *103*, 19512–19517.
9. Tailby, C., Solomon, S.G., Dhruv, N.T., Majaj, N.J., Sokol, S.H., and Lennie, P. (2007). A new code for contrast in the primate visual pathway. J. Neurosci. *27*, 3904–3909.
10. Solomon, S.G., Tailby, C., Cheong, S.K., and Camp, A.J. (2010). Linear and nonlinear contributions to the visual sensitivity of neurons in primate lateral geniculate nucleus. J. Neurophysiol. *104*, 1884–1898.
11. White, A.J.R., Solomon, S.G., and Martin, P.R. (2001). Spatial properties of koniocellular cells in the lateral geniculate nucleus of the marmoset Callithrix jacchus. J. Physiol. *533*, 519–535.
12. Rodieck, R.W., and Dreher, B. (1979). Visual suppression from nondominant eye in the lateral geniculate nucleus: a comparison of cat and monkey. Exp. Brain Res. *35*, 465–477.
13. Pietersen, A.N., Cheong, S.K., Solomon, S.G., Tailby, C., and Martin, P.R. (2014). Temporal response properties of koniocellular (blue-on and blue-off) cells in marmoset lateral geniculate nucleus. J. Neurophysiol. *112*, 1421–1438.
14. Frazor, R.A., and Geisler, W.S. (2006). Local luminance and contrast in natural images. Vision Res. *46*, 1585–1598.
15. Naka, K.-I., and Rushton, W.A. (1966). S-potentials from colour units in the retina of fish (*Cyprinidae*). J. Physiol. *185*, 536–555.
16. Kaas, J.H., Huerta, M.F., Weber, J.T., and Harting, J.K. (1978). Patterns of retinal terminations and laminar organization of the lateral geniculate nucleus of primates. J. Comp. Neurol. *182*, 517–553.
17. Harting, J.K., Huerta, M.F., Hashikawa, T., and van Lieshout, D.P. (1991). Projection of the mammalian superior colliculus upon the dorsal lateral geniculate nucleus: organization of tectogeniculate pathways in nineteen species. J. Comp. Neurol. *304*, 275–306.
18. Casagrande, V.A. (1994). A third parallel visual pathway to primate area V1. Trends Neurosci. *17*, 305–310.
19. Sherk, H. (1979). A comparison of visual-response properties in cat's parabigeminal nucleus and superior colliculus. J. Neurophysiol. *42*, 1640–1655.
20. Tailby, C., Cheong, S.K., Pietersen, A.N., Solomon, S.G., and Martin, P.R. (2012). Colour and pattern selectivity of receptive fields in superior colliculus of marmoset monkeys. J. Physiol. *590*, 4061–4077.
21. Marrocco, R.T., and Li, R.H. (1977). Monkey superior colliculus: properties of single cells and their afferent inputs. J. Neurophysiol. *40*, 844–860.
22. Bishop, P.O., and Pettigrew, J.D. (1986). Neural mechanisms of binocular vision. Vision Res. *26*, 1587–1600.
23. Ohzawa, I., DeAngelis, G.C., and Freeman, R.D. (1997). Encoding of binocular disparity by complex cells in the cat's visual cortex. J. Neurophysiol. *77*, 2879–2909.
24. Cheong, S.K., Tailby, C., Solomon, S.G., and Martin, P.R. (2013). Cortical-like receptive fields in the lateral geniculate nucleus of marmoset monkeys. J. Neurosci. *33*, 6864–6876.
25. Xue, J.T., Ramoa, A.S., Carney, T., and Freeman, R.D. (1987). Binocular interaction in the dorsal lateral geniculate nucleus of the cat. Exp. Brain Res. *68*, 305–310.
26. Mysore, S.P., and Knudsen, E.I. (2013). A shared inhibitory circuit for both exogenous and endogenous control of stimulus selection. Nat. Neurosci. *16*, 473–478.
27. Gruberg, E., Dudkin, E., Wang, Y., Marín, G., Salas, C., Sentis, E., Letelier, J., Mpodozis, J., Malpeli, J., Cui, H., et al. (2006). Influencing and interpreting visual input: the role of a visual feedback system. J. Neurosci. *26*, 10368–10371.
28. Hendry, S.H.C., and Yoshioka, T. (1994). A neurochemically distinct third channel in the macaque dorsal lateral geniculate nucleus. Science *264*, 575–577.
29. Casagrande, V.A., Yazar, F., Jones, K.D., and Ding, Y. (2007). The morphology of the koniocellular axon pathway in the macaque monkey. Cereb. Cortex *17*, 2334–2345.
30. Solomon, S.G. (2002). Striate cortex in dichromatic and trichromatic marmosets: neurochemical compartmentalization and geniculate input. J. Comp. Neurol. *450*, 366–381.
31. Sincich, L.C., Park, K.F., Wohlgemuth, M.J., and Horton, J.C. (2004). Bypassing V1: a direct geniculate input to area MT. Nat. Neurosci. *7*, 1123–1128.
32. Warner, C.E., Goldshmit, Y., and Bourne, J.A. (2010). Retinal afferents synapse with relay cells targeting the middle temporal area in the pulvinar and lateral geniculate nuclei. Front. Neuroanat. *4*, 8.
33. Cruz-Martín, A., El-Danaf, R.N., Osakada, F., Sriram, B., Dhande, O.S., Nguyen, P.L., Callaway, E.M., Ghosh, A., and Huberman, A.D. (2014). A dedicated circuit links direction-selective retinal ganglion cells to the primary visual cortex. Nature *507*, 358–361.
34. Piscopo, D.M., El-Danaf, R.N., Huberman, A.D., and Niell, C.M. (2013). Diverse visual features encoded in mouse lateral geniculate nucleus. J. Neurosci. *33*, 4642–4656.
35. Scholl, B., Latimer, K.W., and Priebe, N.J. (2012). A retinal source of spatial contrast gain control. J. Neurosci. *32*, 9824–9830.
36. Zhao, X., Chen, H., Liu, X., and Cang, J. (2013). Orientation-selective responses in the mouse lateral geniculate nucleus. J. Neurosci. *33*, 12751–12763.
37. Hale, P.T., Sefton, A.J., and Dreher, B. (1979). A correlation of receptive field properties with conduction velocity of cells in the rat's retino-geniculo-cortical pathway. Exp. Brain Res. *35*, 425–442.
38. Grubb, M.S., and Thompson, I.D. (2003). Quantitative characterization of visual response properties in the mouse dorsal lateral geniculate nucleus. J. Neurophysiol. *90*, 3594–3607.
39. Dick, A., Kaske, A., and Creutzfeldt, O.D. (1991). Topographical and topological organization of the thalamocortical projection to the striate and prestriate cortex in the marmoset (Callithrix jacchus). Exp. Brain Res. *84*, 233–253.
40. Sefton, A.J., Dreher, B., Harvey, A.R., and Martin, P.R. (2014). Visual system. In The Rat Nervous System, G. Paxinos, ed. (Elsevier Academic Press), pp. 947–983.
41. Fitzpatrick, D., Itoh, K., and Diamond, I.T. (1983). The laminar organization of the lateral geniculate body and the striate cortex in the squirrel monkey (*Saimiri sciureus*). J. Neurosci. *3*, 673–702.
42. Gamlin, P.D. (2006). The pretectum: connections and oculomotor-related roles. Prog. Brain Res. *151*, 379–405.
43. Sherman, S.M., and Guillery, R.W. (2006). Exploring the Thalamus and Its Role in Cortical Function (MIT Press).

